AGU PUBLICATIONS

Geophysical Research Letters

Key Points:
- UV-driven loss of snow nitrate determines its N isotopes in different climates
- Fractional loss of snow nitrate was up to 50% in the ice age at Summit Greenland
- Nitrate depositional flux to Greenland in the last ice age is ~40% lower than in the Holocene

Supporting Information:
- Texts S1–S3, Table S1, and Data Set S1

Correspondence to:
L. Geng,
leigeng@uw.edu

Effects of postdepositional processing on nitrogen isotopes of nitrate in the Greenland Ice Sheet Project 2 ice core

Lei Geng[1], Maria C. Zatko[1], Becky Alexander[1], T. J. Fudge[2], Andrew J. Schauer[2], Lee T. Murray[3,4], and Loretta J. Mickley[5]

[1]Department of Atmospheric Sciences, University of Washington, Seattle, Washington, USA, [2]Department of Earth and Space Sciences, University of Washington, Seattle, Washington, USA, [3]NASA Goddard Institute for Space Studies, New York, New York, USA, [4]Lamont-Doherty Earth Observatory, Columbia University, Palisades, New York, USA, [5]School of Engineering and Applied Sciences, Harvard University, Cambridge, Massachusetts, USA

Abstract Records of ice core nitrate and its isotopes hold the potential to assess past atmospheric conditions regarding NO_x and oxidant levels. However, relating such records to past atmospheric conditions requires a site-specific understanding of the postdepositional processing of snow nitrate. We report $\delta^{15}N(NO_3^-)$ records from the Greenland Ice Sheet Project 2 (GISP2) ice core over major climate transitions. Model calculations and comparison with records of parameters influencing UV-driven postdepositional processing of snow nitrate suggest that the observed variability in GISP2 $\delta^{15}N(NO_3^-)$ over major climate transitions is primarily driven by changes in the degree of postdepositional loss of snow nitrate. Estimates of the fractional loss of snow nitrate is (16–23)% in the Holocene and (45–53)% in the glacial period, suggesting a (41 ± 32)% lower nitrate depositional flux to Greenland during the glacial period relative to the Holocene.

1. Introduction

Nitrate (NO_3^-) is one of the most abundant ions measured in polar snow and ice cores. Chronologic records of ice core nitrate concentrations and its stable isotopic composition ($\delta^{15}N$, $\delta^{18}O$, and $\Delta^{17}O$, where $\delta = R_{\text{sample}}/R_{\text{reference}} - 1$ and $\Delta^{17}O = \delta^{17}O - 0.52 \times \delta^{18}O$, with R denoting the $^{15}N/^{14}N$, $^{18}O/^{16}O$, and $^{17}O/^{16}O$ ratios, and the reference is N_2-AIR for nitrogen and Vienna Standard Mean Ocean Water for oxygen) have the potential to assess past atmospheric abundance and/or source variability of NO_x [*Hastings et al.*, 2005; *Mayewski et al.*, 1990] and the tropospheric oxidative capacity [*Alexander and Mickley*, 2015; *Alexander et al.*, 2004]. However, relating ice core records of nitrate and its isotopic signatures to past atmospheric conditions must rely on an understanding of site-specific effects of postdepositional processing on snow nitrate concentration and its isotopes [*Morin et al.*, 2009].

The postdepositional processing of snow nitrate is a complex process occurring in the air-snow interface, initiated mainly by ultraviolet (UV) photolysis of snow nitrate [*Erbland et al.*, 2013; *Frey et al.*, 2009]. The main photoproduct, NO_x, can be transported from the snowpack to the overlying atmosphere [*Honrath et al.*, 1999; *Thomas et al.*, 2012; *Zatko et al.*, 2013], where it is reoxidized to nitrate and subsequently redeposited to the snow surface or transported away [*Davis et al.*, 2004]. That snow-sourced NO_x/nitrate transported away from its site of emission represents a loss of nitrate from the snowpack, making interpretation of ice core nitrate concentrations in terms of past atmospheric nitrate and NO_x abundance difficult [*Wolff et al.*, 2008]. In addition to disturbing the preservation of nitrate concentrations in ice cores, postdepositional processing also alters its nitrogen and oxygen isotopic composition [*Blunier et al.*, 2005; *Erbland et al.*, 2013; *Frey et al.*, 2009]. The large fractionation constants (ε) associated with nitrate photolysis ($^{15}\varepsilon = (-47.9 \pm 6.8)$‰ [*Berhanu et al.*, 2014] and $^{18}\varepsilon = -34$‰ [*Frey et al.*, 2009]) tend to increase $\delta^{15}N$ and $\delta^{18}O$ of nitrate remaining in the snow, but $\Delta^{17}O$ of that would not be influenced as only mass-dependent fractionation is induced by photolysis. Following photolysis, the recycling of nitrate in the condensed phase of snow grains and at the air-snow interface alters snow $\delta^{18}O(NO_3^-)$, $\Delta^{17}O(NO_3^-)$, and the depth profile of $\delta^{15}N(NO_3^-)$ in surface snow [*Erbland et al.*, 2013; *Frey et al.*, 2009], but the depth-integrated $\delta^{15}N(NO_3^-)$ in snow and ice will remain intact unless net loss of snow nitrate occurs. This makes $\delta^{15}N(NO_3^-)$ a more reliable proxy than $\delta^{18}O(NO_3^-)$ for estimating the degree of postdepositional loss of snow nitrate.

The degree of postdepositional processing of snow nitrate is influenced mainly by surface UV intensity, snow accumulation rate, snow UV light-absorbing impurities (UV-LAI) (e.g., organics, dust, and black carbon), and snow grain size and shape [*France et al.*, 2011; *Frey et al.*, 2009; *Libois et al.*, 2013; *Zatko et al.*, 2013]. Given constant UV radiation, the degree of postdepositional processing of snow nitrate depends on the time (T_z) nitrate spends in the snow's photic zone (30–90 cm deep [*Erbland et al.*, 2013; *France et al.*, 2011; *Zatko et al.*, 2013]). The depth of the photic zone is determined by concentrations of snow UV-LAI, and T_z is determined by local snow accumulation rate. Due to the high snow accumulation rate at Summit, Greenland (0.24 m ice a^{-1} accumulation), the degree of postdepositional processing is thought to be small and thus atmospheric signals of nitrate and its isotopes are preserved [*Fibiger et al.*, 2013; *Hastings et al.*, 2004]. However, these studies at Summit cover short time periods (several months to a few years) when the snow accumulation rate is relatively constant, so that the effect of postdepositional processing on snow nitrate and its isotopes is difficult to isolate from other processes such as atmospheric variability in NO$_x$ sources [*Hastings et al.*, 2003], NO$_x$ cycling [*Freyer et al.*, 1993], and/or partitioning of nitrate between the gas phase and aerosol phase [*Geng et al.*, 2014]. On longer time scales, e.g., the glacial-interglacial transition, snow accumulation rate, and snow UV-LAI vary significantly [*Cuffey and Clow*, 1997; *Mayewski et al.*, 1997], which may alter the degree of postdepositional processing and impact the preservation of nitrate and its isotopes.

Previous measurements of glacial-interglacial δ^{15}N(NO$_3^-$) at Summit, Greenland, showed δ^{15}N(NO$_3^-$) of (28.4 ± 1.1)‰ and (9.7 ± 0.7)‰ in the glacial period and the Holocene, respectively [*Hastings et al.*, 2005]. This glacial-interglacial difference was attributed to variability in the relative importance of NO$_x$ sources. The effect of postdepositional processing was excluded because ice core δ^{15}N(NO$_3^-$) values at different Greenland sites (e.g., Summit versus Dye 3) do not follow the expected patterns of δ^{15}N(NO$_3^-$) based on differences in local snow accumulation rates [*Hastings et al.*, 2005]. However, the dust concentration is lower at Dye 3 (35 μg L^{-1}) than at Summit (77 μg L^{-1}) [*Bory et al.*, 2003], which tends to counteract the effect of the higher snow accumulation at Dye 3 (0.40 versus 0.24 m ice a^{-1} at Summit). Furthermore, at sites with similar snow accumulation rates, the net loss could be different due to varying local atmospheric conditions (e.g., oxidant concentrations and wind speed and direction) that influence the rates of recycling and export of snow-sourced NO$_x$. *Morin et al.* [2009] also noted that no natural NO$_x$ source carries a strongly positive δ^{15}N signature which is necessary to explain the high δ^{15}N(NO$_3^-$) values observed in GISP2 in terms of NO$_x$ source-driven variability and suggested that changes in postdepositional processing could be responsible for the observed glacial-interglacial difference in δ^{15}N(NO$_3^-$) by *Hastings et al.* [2005].

In this study, we report new δ^{15}N(NO$_3^-$) data from the GISP2 ice core covering the glacial-interglacial cycle and two abrupt climate change cycles during the last glacial period (i.e., the Dansgaard-Oeschger (D-O) cycles [*Dansgaard et al.*, 1993]). We compare the new measurements to previous estimates of snow accumulation rate and with indicators of snow UV-LAI in order to assess the potential effects of postdepositional loss on the ice core δ^{15}N(NO$_3^-$) record. The implications of postdepositional processing of snow nitrate for the interpretation of ice core records of nitrate concentration and its isotopes in central Greenland over major climate transitions are discussed.

2. Method

2.1. Sample Collection

We collected 15 discrete samples (~2 kg of ice each) from the GISP ice core (drilled at Summit, Greenland, 72.6°N, 38.5°W, 3200 m elevation, 0.24 m ice a^{-1} at present [*Cuffey and Clow*, 1997]) between 264 and 2735 m depth covering the last glacial-interglacial cycle (~1 to 100 ka B.P.). Each sample spans ~50 cm depth, representing 2–200 years of snow accumulation. We also collected 112 continuous samples throughout the depth interval of 2310 to 2413 m, covering the D-O 12 and 13 cycles between 43 and 49 ka B.P. [*Grootes and Stuiver*, 1997]. The length of each sample is 0.8–1.0 m, representing 50–60 years of snow accumulation.

In the IsoLab (http://isolab.ess.washington.edu/isolab/) at the University of Washington, all samples were decontaminated by removing the surface layer (~0.5 cm) with a band saw in a cold room (−8°C) followed by rinsing with 18 MΩ cm water. The samples were then placed in covered, precleaned beakers and
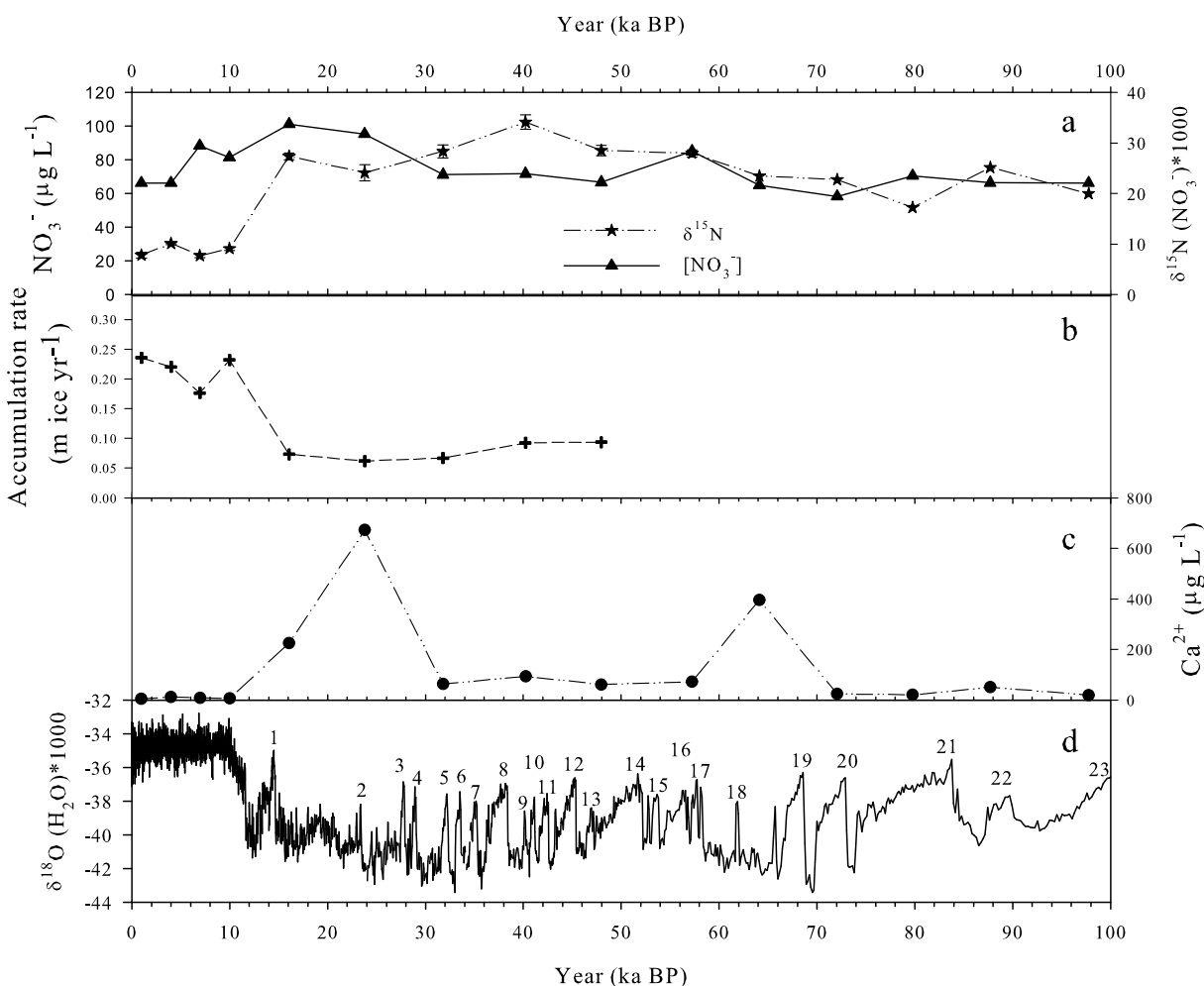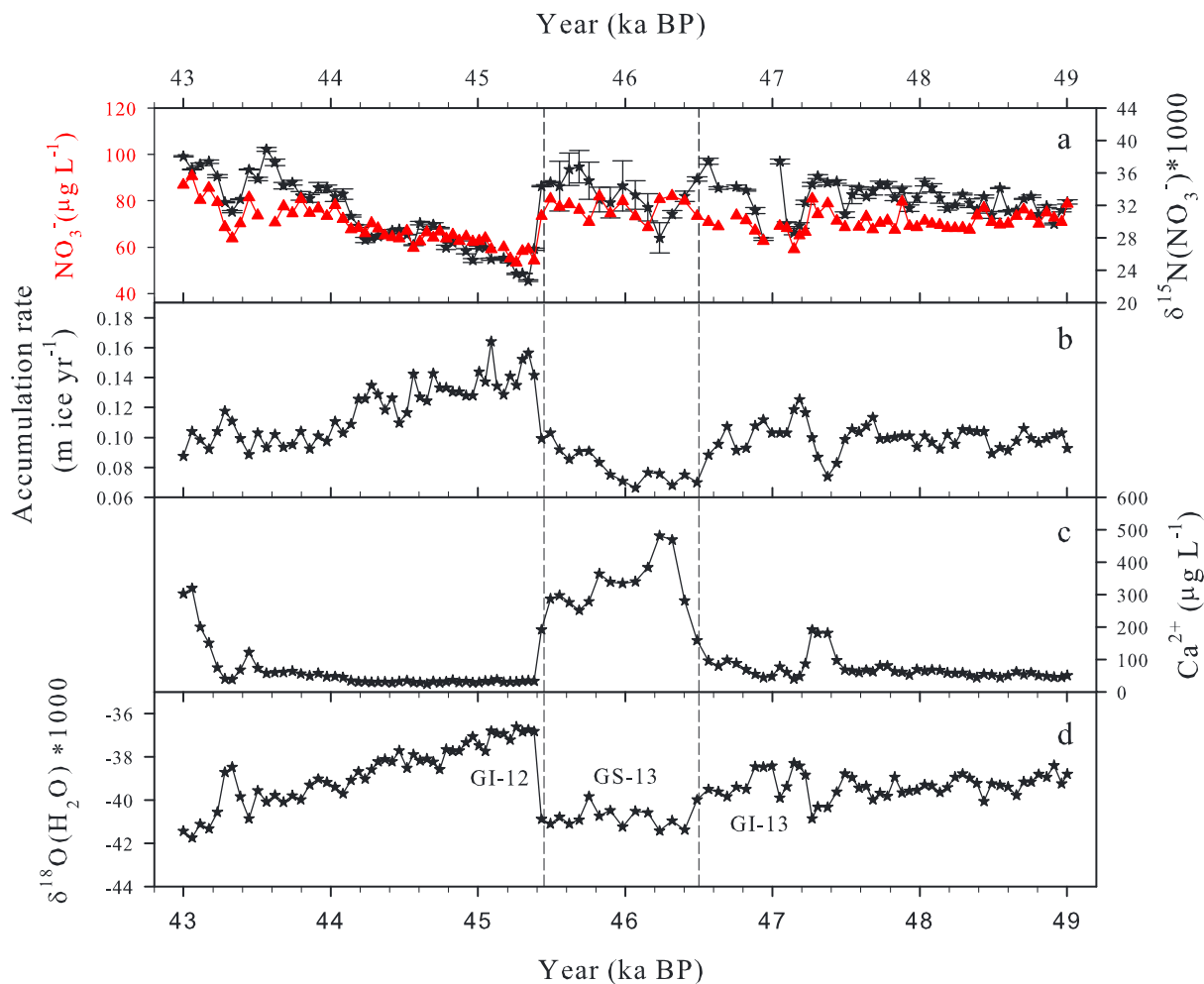
Figure 1. Records of (a) concentration and $\delta^{15}N$ of NO_3^-, (b) snow accumulation rate, (c) Ca^{2+} concentrations, and (d) the high-resolution record of $\delta^{18}O$ of water in the GISP2 ice core. Numbers in Figure 1d represent the 23 abrupt climate change (D-O) events in the past 100 ka. Concentrations of NO_3^- and Ca^{2+} and snow accumulation rate are the means in the depth interval of each sample in this study estimated from the high-resolution data in *Mayewski et al.* [1997] and *Cuffey and Clow* [1997] (the snow accumulation rate data only extend to ~50 ka B.P.), respectively. The $\delta^{18}O$ of water data and timescale used are both from *Grootes and Stuiver* [1997].

melted at room temperature in a clean, laminar flow hood. The mean concentration of NO_3^- and Ca^{2+} (representing dust) of each sample was determined by calculating their mean concentrations over the depth of each sample from the high-resolution records of *Mayewski et al.* [1997]. The mean snow accumulation rate for each sample was calculated based on the high-resolution record of snow accumulation rate (m ice a^{-1}) reconstructed by *Cuffey and Clow* [1997]. Concentrations of snow UV-LAI other than dust (e.g., organics and black carbon) likely vary only slightly between the glacial and interglacial climate based on observations of organic acids and ammonium which are proxies for biomass and fire emissions [*Fuhrer and Legrand*, 1997].

2.2. Nitrate Isotope Analysis

Nitrogen isotopes of above samples were measured in triplicate in the University of Washington IsoLab using the denitrifier method [*Sigman et al.*, 2001] both with and without the gold tube [*Kaiser et al.*, 2007] on a Delta Advantage isotope ratio mass spectrometer. Briefly, denitrifying bacteria convert NO_3^- to N_2O which is either measured directly or decomposed to O_2 and N_2 in a heated gold tube. The $\delta^{15}N$ values were calibrated against two international standards USGS34 ($\delta^{15}N = -1.8‰$) and USGS32 ($\delta^{15}N = 180‰$) [*Bohlke et al.*, 1993; *Kaiser et al.*, 2007]. Another international standard, IAEA-NO-3 with $\delta^{15}N = 4.7‰$, was used as a quality control. The standard deviation of $\delta^{15}N$ for the discrete samples was $\pm 0.25‰$ as indicated by

Figure 2. Records of (a) concentration and $\delta^{15}N$ of NO_3^-, (b) snow accumulation rate, (c) Ca^{2+} concentrations, and (d) high-resolution record of $\delta^{18}O$ of water in the GISP2 ice core during the D-O 12 and 13 cycles. The concentration, snow accumulation rate, and $\delta^{18}O$ of water are from the same sources as Figure 1. GS and GI are the cold and warm phases in the D-O cycles, respectively.

repeated measurements of IAEA-NO-3 and that for the continuous samples was ±0.25‰ as indicated by repeated measurements USGS32. Details on sample preparation and the analytical procedures are given in Text S1 in the supporting information.

3. Results

Figures 1 and 2 show $\delta^{15}N(NO_3^-)$, the mean concentrations of NO_3^- and Ca^{2+}, and snow accumulation rate (A) as a function of $\delta^{18}O$ of water in GISP2 [*Grootes and Stuiver*, 1997] over the last glacial-interglacial cycle, and the D-O 12 and 13 cycles, respectively. $\delta^{15}N(NO_3^-)$ in the last glacial period was (25.3 ± 4.6)‰, higher than in the Holocene ((8.6 ± 1.3)‰). The glacial-interglacial difference ((16.7 ± 4.8)‰) is comparable with previous measurements (18.7‰) [*Hastings et al.*, 2005]. There is no significant glacial-interglacial difference in nitrate concentrations, as also indicated by the high-resolution record [*Mayewski et al.*, 1997]. There are large differences in snow accumulation rate (0.16 m ice a^{-1} difference) and Ca^{2+} concentrations (~215.3 $\mu g\,L^{-1}$ difference) on this time scale.

During the D-O 12 and 13 cycles (43–49 ka B.P., Figure 2), $\delta^{15}N(NO_3^-)$ displays an apparent trend with temperatures showing lower values in warmer climates, consistent with the observed glacial-interglacial variability. The mean $\delta^{15}N(NO_3^-)$ in this period was (31.8 ± 3.5)‰. The full magnitude of the variability in

$\delta^{15}N(NO_3^-)$ in this period was 16.2‰. The snow accumulation rate and Ca^{2+} concentration also varied significantly (0.07–0.16 m ice a^{-1} and 24.8–481.3 µg L^{-1}, respectively). Unlike the relatively stable nitrate concentrations between the discrete samples in the Holocene ((74 ± 11) µg L^{-1}) and last glacial period ((75 ± 14) µg L^{-1}), nitrate concentrations during these two D-O cycles decreased with increasing temperature, similar to $\delta^{15}N(NO_3^-)$.

4. Discussion

### 4.1. Glacial-Interglacial Variations in $\delta^{15}N(NO_3^-)$ in GISP2

$\delta^{15}N$ signatures of the main natural NO_x sources (i.e., biomass burning, lightning, and soil emissions [*Levy et al.*, 1999]) are different (-9‰ to ~0, references in *Geng et al.* [2014]), and thus, variations in NO_x sources could leave signatures on the ice core $\delta^{15}N(NO_3^-)$ record. However, for the proportional contributions of NO_x sources to cause the observed ~17‰ glacial-interglacial $\delta^{15}N(NO_3^-)$ difference, $\delta^{15}N$ signatures of the main natural NO_x sources must differ by more than 17‰. This is very unlikely on the basis of current measurements of $\delta^{15}N$ on NO_x sources as summarized in *Geng et al.* [2014]. Although stratospheric nitrate contributes to snow nitrate in Antarctica and is expected to possess $\delta^{15}N$ of (19 ± 3)‰ [*Savarino et al.*, 2007], it is a much weaker nitrate source than those of tropospheric origins [*Lee et al.*, 2014] and has not been observed to be significant for Arctic snow nitrate.

Before deposition to the snow surface, NO_x recycling [*Freyer et al.*, 1993] and atmospheric nitrate partitioning between the gas phase and aerosol phase [*Geng et al.*, 2014; *Heaton et al.*, 1997] could also lead to variations in $\delta^{15}N(NO_3^-)$. In particular, variations in O_3 and HO_2/RO_2 concentrations will shift the ratio of NO/NO_2, where nitrogen isotope fractionation alters $\delta^{15}N(NO_2)$ and thus $\delta^{15}N(NO_3^-)$. Following the approximations in *Geng et al.* [2014], we calculate that glacial $\delta^{15}N(NO_3^-)$ can be ~1‰ higher than in the Holocene due to the predicted 20% decrease in glacial tropospheric ozone abundance from the Holocene [*Murray et al.*, 2014]. Regarding the effect of gas/aerosol partitioning of atmospheric nitrate, assuming all nitrate stays in the aerosol phase during the glacial period due to the general alkaline conditions resulting from high sea salt and dust concentrations [*Mayewski et al.*, 1997], the model in *Geng et al.* [2014] indicates ~10‰ increase in glacial $\delta^{15}N(NO_3^-)$. This is the upper limit based on the maximum difference in the gas-phase fraction of nitrate (f_g) transported and deposited to Summit between the Holocene ($f_g = \sim 45\%$, using the preindustrial value estimated in *Geng et al.* [2014]) and the last glacial period ($f_g \approx 0\%$). Although the change induced by the gas-particle partitioning of nitrate is in the same direction as the observations, it cannot account for the full magnitude of the observed difference (~17‰).

The high $\delta^{15}N(NO_3^-)$ values in the Holocene ((8.6 ± 1.3)‰) and the last glacial period ((25.3 ± 4.6)‰) relative to $\delta^{15}N$ of natural NO_x sources (<0‰) suggest some degree of postdepositional loss of snow nitrate at Summit, consistent with *Dibb et al.* [2007], *Morin et al.* [2009], and *Geng et al.* [2014]. Assuming $\delta^{15}N(NO_3^-)$ originally deposited to the snow is 0‰, which is within the range of observed atmospheric $\delta^{15}N(NO_3^-)$ of (-4.5 ± 5.4)‰ most representative of natural background tropospheric nitrate [*Savarino et al.*, 2007], the Holocene $\delta^{15}N(NO_3^-)$ indicates ~16% net loss of nitrate from the snowpack estimated from the Rayleigh-type fractionation model [*Blunier et al.*, 2005] with a fractionation constant of -47.9‰ [*Berhanu et al.*, 2014]. This level of loss is within the range (5–25%) estimated by *Dibb et al.* [2007] based on concentration measurements.

The lower glacial snow accumulation rate than the Holocene (0.08 versus 0.21 m ice a^{-1}) suggests potential for a larger degree of postdepositional loss, qualitatively consistent with the enriched glacial $\delta^{15}N(NO_3^-)$. To estimate the increase in postdepositional loss during the glacial period relative to the Holocene, we use the parameterization from *Zatko et al.* [2013] to calculate actinic flux within the snow photic zone and T_z in the two periods (Text S2), with mean dust concentrations listed in Table S1. The snow accumulation rate data do not extend prior to ~50 ka B.P. [*Cuffey and Clow*, 1997], so in the following discussion we only consider the glacial $\delta^{15}N(NO_3^-)$ data younger than 50 ka B.P. with a mean of (28.5 ± 3.6)‰. Snow concentrations of organics and black carbon are assumed to be constant between the glacial and interglacial periods, though limited ice core records indicate that they are slightly lower in the glacial period [*Fuhrer and Legrand*, 1997]. The model result indicates that T_z changes from 0.67 to 1.83 year from the Holocene to the last glacial period, a factor of 2.74 increase in the time that nitrate remains in the
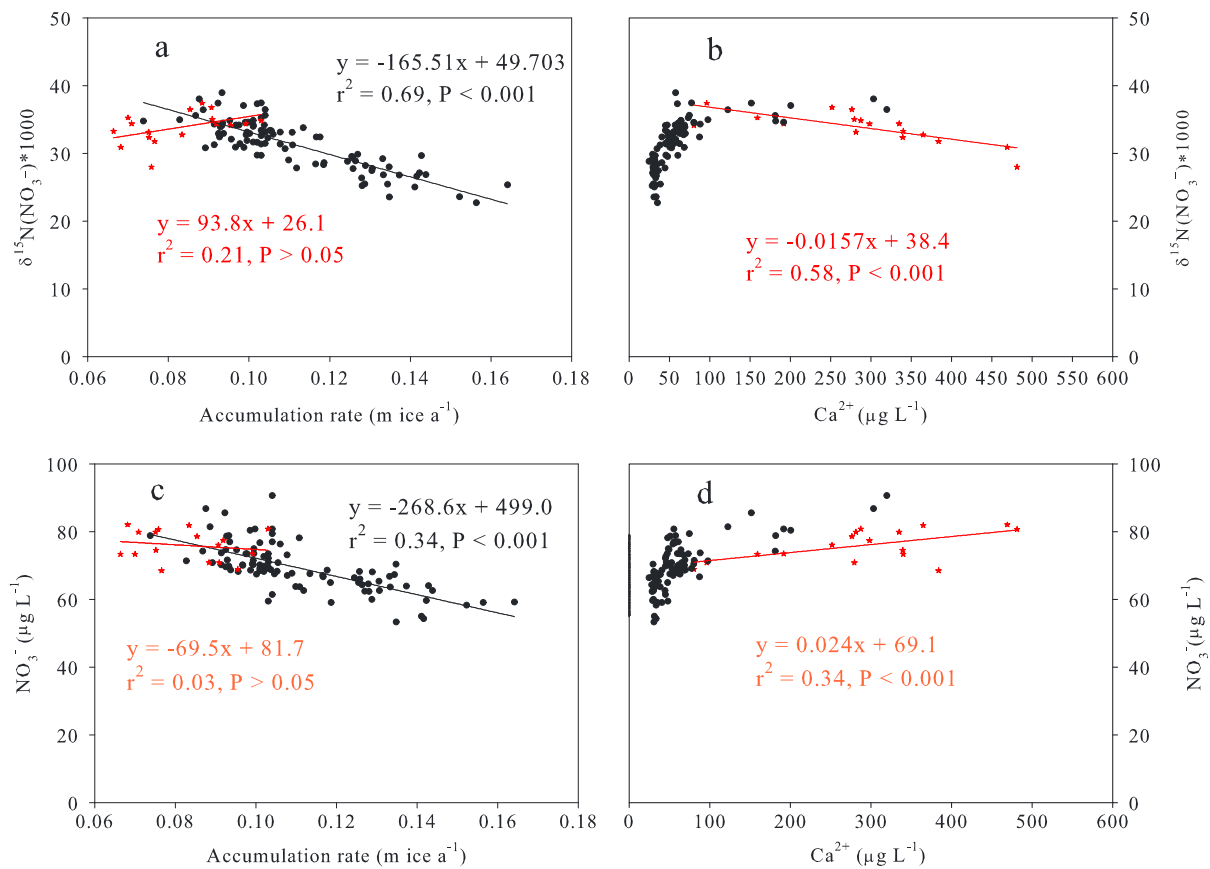
Figure 3. $\delta^{15}N(NO_3^-)$ versus (a) snow accumulation rate and (b) Ca^{2+} concentration. NO_3^- concentration versus (c) snow accumulation rate and (d) Ca^{2+} concentration in the two D-O cycles from 43 to 49 ka B.P. Red dots in each subfigure represent samples in GS-13 (45.4–46.6 ka B.P.), while black dots are those before and after GS-13.

snow photic zone. Assuming the same factor of increase in net nitrate loss, loss of snow nitrate in the glacial period would have been ~45% compared to 16% in the Holocene. This 45% net loss would lead to glacial $\delta^{15}N(NO_3^-)$ of 27.5‰ according to the Rayleigh-type fractionation model. This, compared to the observed average of (28.5 ± 3.6)‰ during 16–50 ka B.P., suggests that changes in $\delta^{15}N(NO_3^-)$ originating from variations in the degree of postdepositional loss of snow nitrate alone can fully account for the glacial-interglacial $\delta^{15}N(NO_3^-)$ difference. We note that the model calculations have uncertainties originating from assumptions such as constant actinic flux between the different climates. In Text S3, we discuss the most important uncertain factors and their impacts on our calculations.

The estimated fractional loss in each time period is dependent upon the $\delta^{15}N$ of nitrate originally deposited to the snow, and on the nitrogen isotope fractionation constant during photolysis, both of which are uncertain. Using the range of $\delta^{15}N(NO_3^-)$ observed in the pristine atmosphere (−7.1‰ to −1.6‰) by one study [*Morin et al.*, 2009], instead of assuming it is 0‰ as in the above calculation, the calculated range of fractional loss is 19–28% and 46–53% in the Holocene and the glacial period, respectively. Using a fractional loss of 16% and 45%, we calculate the original nitrate concentrations before postdepositional loss in the GISP2 ice core of (89.8 ± 13.3) $\mu g\,L^{-1}$ and (147.5 ± 28.7) $\mu g\,L^{-1}$ in the Holocene and the glacial period, respectively. Taking into account the ~65% decrease in the snow accumulation rate during the glacial period relative to the Holocene, we estimate a (41 ± 32) % lower depositional flux of nitrate to Greenland in the glacial period relative to the preindustrial Holocene. Assuming that the originally deposited $\delta^{15}N(NO_3^-)$ was 10‰ (instead of 0‰) due to the potential effect of glacial-interglacial changes in the gas-aerosol partitioning of nitrate, the fractional loss of nitrate in the glacial period would be ~32%. The original glacial nitrate concentration would then be (119.3 ± 23.6) $\mu g\,L^{-1}$, suggesting a (52 ± 27)% lower nitrate depositional flux to Greenland in the glacial period relative to the Holocene.

4.2. GISP2 $\delta^{15}N(NO_3^-)$ During the D-O 12 and 13 Cycles

During the D-O 12 and 13 cycles (43–49 ka B.P.), $\delta^{15}N(NO_3^-)$ decreased with increasing temperature and varied from 22.7‰ to 38.9‰ (Figures 2a and 2d). Around 45.4 ka B.P. when an abrupt warming began, $\delta^{15}N(NO_3^-)$ decreased rapidly by (10.2 ± 2.3)‰ (the difference between the mean $\delta^{15}N(NO_3^-)$ during GS-13 (Greenland stadial, the cold phase of the D-O cycles [*Rasmussen et al.*, 2014]) and the peak of GI-12 (Greenland interstadial, the warm phase of the D-O cycle). During most of the period of the D-O 12 and 13 cycles, $\delta^{15}N$ (NO_3^-) decreased with increasing snow accumulation rate, consistent with the glacial-interglacial variability. However, during GS-13, $\delta^{15}N(NO_3^-)$ does not vary with snow accumulation rate but instead decreases with increasing dust concentrations (Figures 2a–2c). Given the relatively small difference in $\delta^{15}N$ of natural NO_x sources and the small nitrogen isotope fractionation effect associated with NO_x cycling as discussed earlier, changes in the proportional contributions of different NO_x sources and in the NO/NO_2 ratio are unlikely to be responsible for the full magnitude of the observed $\delta^{15}N(NO_3^-)$ variability during the D-O 12 and 13 cycles (16.2‰). Regarding the isotopic effect associated with atmospheric nitrate partitioning between the gas phase and aerosol phase, it is likely insignificant within the D-O cycles because the atmosphere was alkaline throughout this time period, so that aerosol-phase nitrate was always favored.

Alternatively, the covariations in $\delta^{15}N(NO_3^-)$ with snow accumulation rate and/or dust concentrations suggest potential effects of postdepositional processing. As there is no available data for the organic and black carbon content on this time scale, we assume that their concentrations were relatively constant between 43 and 49 ka B.P. Figures 3a and 3b compares $\delta^{15}N(NO_3^-)$ with snow accumulation rate and dust concentrations during these two rapid climate change cycles. Before and after the GS-13 event, when snow accumulation rate was relatively high ((0.11 ± 0.2) m ice a^{-1}) but dust concentrations were low and relatively constant ((50.9 ± 18.7) μg L^{-1}), $\delta^{15}N(NO_3^-)$ is negatively correlated with snow accumulation rate ($r^2 = 0.69$, $P < 0.001$) and shows no linear correlation with dust. This suggests that changes in snow accumulation rate-controlled variability in postdepositional loss and thus $\delta^{15}N(NO_3^-)$ during this period. In GS-13, when the snow accumulation rate was relatively low ((0.08 ± 0.1) m ice a^{-1}), but dust concentrations were high and highly variable ((315.9 ± 88.1) μg L^{-1}), $\delta^{15}N(NO_3^-)$ became negatively correlated with dust concentrations ($r^2 = 0.58$, $P < 0.001$) and showed no significant correlation with snow accumulation rate. This in turn suggests the dominance of UV-LAI on variability in the degree of postdepositional loss of snow nitrate and thus $\delta^{15}N$ (NO_3^-) during GS-13 though its impacts on the depth of the snow photic zone. The effect of dust on the location of nitrate in snow grains may be also important [*Meusinger et al.*, 2014]; however, we do not yet have enough information to quantify this effect. *Erbland et al.* [2013] observed a relationship between ln $(\delta^{15}N(NO_3^-) + 1)$ and 1/A with a slope of (5.76 ± 0.47) in Antarctic snow pits. In comparison, the slope of ln $(\delta^{15}N(NO_3^-) + 1)$ versus 1/A in the GISP2 samples during the two D-O cycles, except those in GS-13, is ~ 1.80, suggesting a lower sensitivity of snow $\delta^{15}N(NO_3^-)$ to snow accumulation rate in Greenland compared to Antarctica. This is likely due to the higher snow UV-LAI concentrations in Greenland than in Antarctica [*Zatko et al.*, 2013], which may lower the sensitivity of $\delta^{15}N(NO_3^-)$ to snow accumulation rate.

As described in the previous section, we use the parameterizations from *Zatko et al.* [2013] to calculate actinic flux and T_z in the snow photic zone before and after the abrupt warming ~ 45.4 ka B.P. with respect to changing snow accumulation rate ((0.08 ± 0.1) m ice a^{-1} to (0.15 ± 0.01) m ice a^{-1}) and dust concentrations ((315.9 ± 88.1) μg L^{-1} to (34.2 ± 0.8) μg L^{-1} (Table S1). The results indicate T_z is 1.67 and 0.99 year before and after the abrupt warming. This change in T_z (a factor of ~1.68) suggests a ~ 12‰ difference in $\delta^{15}N$ (NO_3^-), comparable to the observed (10.2 ± 2.3)‰ rapid change at this time. However, although the magnitude of the calculated change is consistent with the observations, the modeled $\delta^{15}N(NO_3^-)$ values before and after the abrupt warming are approximately 10‰ lower than the observations (Table S1). This discrepancy may be due to overestimates in the reconstructed snow accumulation rates at Summit during this period. Uncertainties in many other factors may also contribute, including the concentration of snow organic impurities, snow pH, location of nitrate in snow grains, snow grain size and shape, and solar irradiance, as discussed in Text S3.

Variations in nitrate concentrations in the D-O 12 and 13 cycles also suggest an impact from postdepositional processing at Summit in the past climate. Figures 3c and 3d shows that in general, snow nitrate concentration is negatively correlated with snow accumulation rate ($r^2 = 0.34$, $P < 0.001$), as more snowfall dilutes nitrate in surface snow. However, during GS-13 when the snow accumulation rate was very low, the statistical

relationship between nitrate concentration and snow accumulation rate disappeared. Instead, during GS-13, nitrate concentration became positively correlated with dust concentrations ($r^2 = 0.34$, $P < 0.001$). This is consistent with the role of dust on postdepositional loss of nitrate, when higher dust concentration led to less nitrate loss from the snow due to its absorption of UV radiation.

5. Conclusion and Implications

We present $\delta^{15}N(NO_3^-)$ data from the GISP2 ice core covering the last glacial-interglacial (1–100 ka B.P.) and two D-O cycles (43–49 ka B.P.). Examination of factors influencing ice core $\delta^{15}N(NO_3^-)$ suggests that changes in the degree of postdepositional processing of snow nitrate, dominated by variations in snow accumulation rate, is likely the primary factor leading to the observed glacial-interglacial $\delta^{15}N(NO_3^-)$ difference. Model calculations of changes in the time that nitrate remains in the snow photic zone between the glacial and interglacial periods also indicate that variations in the degree of postdepositional loss alone can fully account for the magnitude of the observed $\delta^{15}N(NO_3^-)$ difference. Variations in gas/aerosol partitioning of atmospheric nitrate could also contribute to up to ~ 50% of the observed glacial-interglacial $\delta^{15}N(NO_3^-)$ difference. During the D-O 12 and 13 cycles between 43 and 49 ka B.P., varying degree of postdepositional loss with climate change is also the primary factor driving the observed variations in $\delta^{15}N(NO_3^-)$. During most of the D-O 12 and 13 cycles, changes in the snow accumulation rate dominate variability in postdepositional loss of snow nitrate and in $\delta^{15}N(NO_3^-)$. However, during GS-13, the effect of snow accumulation rate is muted by other factors influencing UV photolysis of snow nitrate, such as variability in the concentrations of snow UV-LAI. Our results and analysis suggest that $\delta^{15}N(NO_3^-)$ in the GISP2 ice core likely carries very limited information on past variability of the relative importance of different sources of NO_x to the atmosphere.

The observed $\delta^{15}N(NO_3^-)$ values indicate a larger UV-induced fractional loss of snowpack nitrate in the glacial period (45–53%) compared to the Holocene (16–28%), suggesting a (41 ± 32%) lower nitrate depositional flux to Greenland in the glacial period relative to the Holocene. These estimated changes are consistent with the 60% (49–67%) glacial-interglacial variability calculated in a chemistry-climate model [*Murray et al*., 2014]. In that study, two thirds of the decrease in nitrate deposition to Summit in the glacial climate is attributable to meteorological changes in the frequency of deposition events, and one third due to decreases in upwind NO_x emissions, the latter of which is highly sensitive to assumptions about biomass burning in the model.

References

Alexander, B., and L. Mickley (2015), Paleo-perspectives on potential future changes in the oxidative capacity of the atmosphere due to climate change and anthropogenic emissions, *Curr. Pollut. Rep.*, 1–13, doi:10.1007/s40726-015-0006-0.

Alexander, B., J. Savarino, K. J. Kreutz, and M. H. Thiemens (2004), Impact of preindustrial biomass-burning emissions on the oxidation pathways of tropospheric sulfur and nitrogen, *J. Geophys. Res.*, 109, D08303, doi:10.1029/2003JD004218.

Berhanu, T. A., C. Meusinger, J. Erbland, R. Jost, S. K. Bhattacharya, M. S. Johnson, and J. Savarino (2014), Laboratory study of nitrate photolysis in Antarctic snow. II. Isotopic effects and wavelength dependence, *J. Chem. Phys.*, 140(24), doi:10.1063/1.4882899.

Blunier, T., G. L. Floch, H. W. Jacobi, and E. Quansah (2005), Isotopic view on nitrate loss in Antarctic surface snow, *Geophys. Res. Lett.*, 32, L13501, doi:10.1029/2005GL023011.

Bohlke, J. K., C. J. Gwinn, and T. B. Coplen (1993), New reference materials for nitrogen-isotope-ratio measurements, *Geostand. Newsl.*, 17(1), 159–164, doi:10.1111/j.1751-908X.1993.tb00131.x.

Bory, A. J. M., P. E. Biscaye, A. M. Piotrowski, and J. P. Steffensen (2003), Regional variability of ice core dust composition and provenance in Greenland, *Geochem. Geophys. Geosyst.*, 4(12), 1107, doi:10.1029/2003GC000627.

Cuffey, K. M., and G. D. Clow (1997), Temperature, accumulation, and ice sheet elevation in central Greenland through the last deglacial transition, *J. Geophys. Res.*, 102(C12), 26,383–26,396, doi:10.1029/96JC03981.

Dansgaard, W., et al. (1993), Evidence for general instability of past climate from a 250-kyr ice-core record, *Nature*, 364(6434), 218–220.

Davis, D., G. Chen, M. Buhr, J. Crawford, D. Lenschow, B. Lefer, R. Shetter, F. Eisele, L. Mauldin, and A. Hogan (2004), South Pole NO_x chemistry: An assessment of factors controlling variability and absolute levels, *Atmos. Environ.*, 38(32), 5375–5388, doi:10.1016/j.atmosenv.2004.04.039.

Dibb, J. E., S. I. Whitlow, and M. Arsenault (2007), Seasonal variations in the soluble ion content of snow at Summit. Greenland: Constraints from three years of daily surface snow samples, *Atmos. Environ.*, 41(24), 5007–5019, doi:10.1016/j.atmosenv.2006.12.010.

Erbland, J., W. C. Vicars, J. Savarino, S. Morin, M. M. Frey, D. Frosini, E. Vince, and J. M. F. Martins (2013), Air-snow transfer of nitrate on the East Antarctic Plateau—Part 1: Isotopic evidence for a photolytically driven dynamic equilibrium in summer, *Atmos. Chem. Phys.*, 13(13), 6403–6419, doi:10.5194/acp-13-6403-2013.

Fibiger, D. L., M. G. Hastings, J. E. Dibb, and L. G. Huey (2013), The preservation of atmospheric nitrate in snow at Summit, Greenland, *Geophys. Res. Lett.*, 40, 3484–3489, doi:10.1002/grl.50659.

France, J. L., M. D. King, M. M. Frey, J. Erbland, G. Picard, S. Preunkert, A. MacArthur, and J. Savarino (2011), Snow optical properties at Dome C (Concordia), Antarctica: Implications for snow emissions and snow chemistry of reactive nitrogen, *Atmos. Chem. Phys.*, 11(18), 9787–9801, doi:10.5194/acp-11-9787-2011.

Frey, M. M., J. Savarino, S. Morin, J. Erband, and J. M. F. Martins (2009), Photolysis imprint in the nitrate stable isotope signal in snow and atmosphere of East Antarctica and implications for reactive nitrogen cycling, *Atmos. Chem. Phys.*, 9(22), 8681–8696, doi:10.5194/acp-9-8681-2009.

Freyer, H. D., D. Kley, A. Volzthomas, and K. Kobel (1993), On the interaction of isotopic exchange processes with photochemical-reactions in atmospheric oxides of nitrogen, *J. Geophys. Res.*, 98(D8), 14,791–14,796, doi:10.1029/93JD00874.

Fuhrer, K., and M. Legrand (1997), Continental biogenic species in the Greenland Ice Core Project ice core: Tracing back the biomass history of the North American continent, *J. Geophys. Res.*, 102(C12), 26,735–26,745, doi:10.1029/97JC01299.

Geng, L., B. Alexander, J. Cole-Dai, E. J. Steig, J. Savarino, E. D. Sofen, and A. J. Schauer (2014), Nitrogen isotopes in ice core nitrate linked to anthropogenic atmospheric acidity change, *Proc. Natl. Acad. Sci. U.S.A.*, 111(16), 5808–5812, doi:10.1073/pnas.1319441111.

Grootes, P. M., and M. Stuiver (1997), Oxygen 18/16 variability in Greenland snow and ice with 10^{-3} to 105-year time resolution, *J. Geophys. Res.*, 102(C12), 26,455–26,470, doi:10.1029/97JC00880.

Hastings, M. G., D. M. Sigman, and F. Lipschultz (2003), Isotopic evidence for source changes of nitrate in rain at Bermuda, *J. Geophys. Res.*, 108(D24), 4790, doi:10.1029/2003JD003789.

Hastings, M. G., E. J. Steig, and D. M. Sigman (2004), Seasonal variations in N and O isotopes of nitrate in snow at Summit, Greenland: Implications for the study of nitrate in snow and ice cores, *J. Geophys. Res.*, 109, D20306, doi:10.1029/2004JD004991.

Hastings, M. G., D. M. Sigman, and E. J. Steig (2005), Glacial/interglacial changes in the isotopes of nitrate from the Greenland Ice Sheet Project 2 (GISP2) ice core, *Global Biogeochem. Cycles*, 19, GB4024, doi:10.1029/2005GB002502.

Heaton, T. H. E., B. Spiro, S. Madeline, and C. Robertson (1997), Potential canopy influences on the isotopic composition of nitrogen and sulphur in atmospheric deposition, *Oecologia*, 109(4), 600–607, doi:10.1007/s004420050122.

Honrath, R. E., M. C. Peterson, and S. Guo (1999), Evidence of NO_x production within or upon ice particles in the Greenland snowpack, *Geophys. Res. Lett.*, 26(6), 695–698, doi:10.1029/1999GL900077.

Kaiser, J., M. G. Hastings, B. Z. Houlton, T. Rockmann, and D. M. Sigman (2007), Triple oxygen isotope analysis of nitrate using the denitrifier method and thermal decomposition of N_2O, *Anal. Chem.*, 79(2), 599–607, doi:10.1021/ac061022s.

Lee, H. M., D. K. Henze, B. Alexander, and L. T. Murray (2014), Investigating the sensitivity of surface-level nitrate seasonality in Antarctica to primary sources using a global model, *Atmos. Environ.*, 89, 757–767, doi:10.1016/j.atmosenv.2014.03.003.

Levy, H., W. J. Moxim, A. A. Klonecki, and P. S. Kasibhatla (1999), Simulated tropospheric NO_x: Its evaluation, global distribution and individual source contributions, *J. Geophys. Res.*, 104(D21), 26,279–26,306, doi:10.1029/1999JD900442.

Libois, Q., G. Picard, J. L. France, L. Arnaud, M. Dumont, C. M. Carmagnola, and M. D. King (2013), Influence of grain shape on light penetration in snow, *Cryosphere*, 7(6), 1803–1818, doi:10.5194/tc-7-1803-2013.

Mayewski, P. A., W. B. Lyons, M. J. Spencer, M. S. Twickler, C. F. Buck, and S. Whitlow (1990), An ice-core record of atmospheric response to anthropogenic sulphate and nitrate, *Nature*, 346, 554–556, doi:10.1038/346554a0.

Mayewski, P. A., L. D. Meeker, M. S. Twickler, S. Whitlow, Q. Z. Yang, W. B. Lyons, and M. Prentice (1997), Major features and forcing of high-latitude northern hemisphere atmospheric circulation using a 110,000-year-long glaciochemical series, *J. Geophys. Res.*, 102(C12), 26,345–26,366, doi:10.1029/96JC03365.

Meusinger, C., T. A. Berhanu, J. Erband, J. Savarino, and M. S. Johnson (2014), Laboratory study of nitrate photolysis in Antarctic snow: I. Observed quantum yield, domain of photolysis, and secondary chemistry, *J. Chem. Phys.*, 140(24), doi:10.1063/1.4882898.

Morin, S., J. Savarino, M. M. Frey, F. Domine, H. W. Jacobi, L. Kaleschke, and J. M. F. Martins (2009), Comprehensive isotopic composition of atmospheric nitrate in the Atlantic Ocean boundary layer from 65 degrees S to 79 degrees N, *J. Geophys. Res.*, 114, D05303, doi:10.1029/2008JD010696.

Murray, L. T., L. J. Mickley, J. O. Kaplan, E. D. Sofen, M. Pfeiffer, and B. Alexander (2014), Factors controlling variability in the oxidative capacity of the troposphere since the Last Glacial Maximum, *Atmos. Chem. Phys.*, 14(7), 3589–3622, doi:10.5194/acp-14-3589-2014.

Rasmussen, S. O., et al. (2014), A stratigraphic framework for abrupt climatic changes during the last glacial period based on three synchronized Greenland ice-core records: Refining and extending the INTIMATE event stratigraphy, *Quat. Sci. Rev.*, 106, 14–28, doi:10.1016/j.quascirev.2014.09.007.

Savarino, J., J. Kaiser, S. Morin, D. M. Sigman, and M. H. Thiemens (2007), Nitrogen and oxygen isotopic constraints on the origin of atmospheric nitrate in coastal Antarctica, *Atmos. Chem. Phys.*, 7(8), 1925–1945, doi:10.5194/acpd-6-8817-2006.

Sigman, D. M., K. L. Casciotti, M. Andreani, C. Barford, M. Galanter, and J. K. Bohlke (2001), A bacterial method for the nitrogen isotopic analysis of nitrate in seawater and freshwater, *Anal. Chem.*, 73(17), 4145–4153, doi:10.1021/ac010088e.

Thomas, J. L., J. E. Dibb, L. G. Huey, J. Liao, D. Tanner, B. L. Lefer, R. von Glasow, and J. Stutz (2012), Modeling chemistry in and above snow at Summit, Greenland—Part 2: Impact of snowpack chemistry on the oxidation capacity of the boundary layer, *Atmos. Chem. Phys.*, 12(14), 6537–6554, doi:10.5194/acp-12-6537-2012.

Wolff, E. W., A. E. Jones, S. J. B. Bauguitte, and R. A. Salmon (2008), The interpretation of spikes and trends in concentration of nitrate in polar ice cores, based on evidence from snow and atmospheric measurements, *Atmos. Chem. Phys.*, 8(18), 5627–5634, doi:10.5194/acp-8-5627-2008.

Zatko, M. C., T. C. Grenfell, B. Alexander, S. J. Doherty, J. L. Thomas, and X. Yang (2013), The influence of snow grain size and impurities on the vertical profiles of actinic flux and associated NO_x emissions on the Antarctic and Greenland ice sheets, *Atmos. Chem. Phys.*, 13(7), 3547–3567, doi:10.5194/acp-13-3547-2013.